Thymic epithelial cells require p53 to support their long-term function in thymopoiesis in mice

Pedro M. Rodrigues,1-3 Ana R. Ribeiro,1-3 Chiara Perrod,1,2 Jonathan J. M. Landry,4 Leonor Ara´ujo,1,2 Isabel Pereira-Castro,1,5 Vladimir Benes,4 Alexandra Moreira,1,5,6 Helena Xavier-Ferreira,1,2 Catarina Meireles,1,2 and Nuno L. Alves1,2

1Instituto de Investigação e Inovação em Saúde, Universidade do Porto, Portugal; 2Thymus Development and Function Laboratory, Instituto de Biologia Molecular e Celular, Porto, Portugal; 3Doctoral Program in Biomedical Sciences, Instituto de Ciências Biomédicas Abel Salazar, Universidade do Porto, Porto, Portugal; 4Genomics Core Facility, European Molecular Biology Laboratory, Heidelberg, Germany; 5Gene Regulation Laboratory, Instituto de Biologia Molecular e Celular, Porto, Portugal; and 6Instituto de Ciências Biomédicas Abel Salazar, Universidade do Porto, Porto, Portugal

Correspondence: Nuno L. Alves, Instituto de Investigação e Inovação em Saude (I3S), Instituto de Biologia Molecular e Celular, Rua Alfredo Allen, 208, 4200-135 Porto, Portugal; e-mail: nalves@ibmc.up.pt.

Originally published in Blood 130(4), 478-488, May 30, 2017.

DOI: 10.1182/blood-2016-12-758961

Key points: • TEC-intrinsic ablation of p53 predominantly affects medullary TECs, altering their RANK-driven differentiation and transcriptome.
• Loss of p53 in TECs couples disrupted thymopoiesis to altered T-cell homeostasis and tolerance

Thymic epithelial cells (TECs) provide crucial microenvironments for T-cell development and tolerance induction. As the regular function of the thymus declines with age, it is of fundamental and clinical relevance to decipher new determinants that control TEC homeostasis in vivo. Beyond its recognized tumor suppressive function, p53 controls several immunoregulatory pathways. To study the cell-autonomous role of p53 in thymic epithelium functioning, we developed and analyzed mice with conditional inactivation of Trp53 in TECs (p53cKO). We report that loss of p53 primarily disrupts the integrity of medullary TEC (mTEC) niche, a defect that spreads to the adult cortical TEC compartment. Mechanistically, we found that p53 controls specific and broad programs of mTEC differentiation. Apart from restraining the expression and responsiveness of the receptor activator of NF-kB (RANK), which is central for mTEC differentiation, deficiency of p53 in TECs altered multiple functional modules of the mTEC transcriptome, including tissuerestricted antigen expression. As a result, p53cKO mice presented premature defects in mTEC-dependent regulatory T-cell differentiation and thymocyte maturation, which progressed to a failure in regular and regenerative thymopoiesis and peripheral T-cell homeostasis in the adulthood. Lastly, peripheral signs of altered immunological tolerance unfold in mutant mice and in immunodeficient mice that received p53cKO-derived thymocytes. Our findings position p53 as a novel molecular determinant of thymic epithelium function throughout life.

Introduction

Within the thymus, thymic epithelial cells (TECs) orchestrate the development of functionally diverse and self-tolerant T cells.[1] Importantly, impaired TEC functions arise with aging, cytoablative regimens and infection, which compromise T-cell responses to pathogens, and vaccination in the elderly, and patients undergoing bone marrow transplantation (BMT) or chemotherapy. Equally, failures in TEC-mediated tolerance induction lead to autoimmunity.[2] Hence, the identification of novel regulators of TEC homeostasis is crucial to comprehend the foundations of immunity and to intervene medically in disorders linked to a dysfunctional thymus.

Cortical TECs (cTECs) and medullary TECs (mTECs) define 2 functionally distinct microenvironments, which differentiate from bipotent TEC progenitors.[1] Whereas cTECs drive T-cell lineage specification and positive selection, mTECs promote the maturation of positively selected thymocytes, regulatory T-cell differentiation, and elimination of autoreactive T cells.[1] Important to mTEC function is their ability to express tissue-restricted antigens (TRA),[2] which depends in part on autoimmune regulator (Aire) and Fezf2.[3,4] Past studies elucidated the role of members of tumor necrosis factor (TNF) receptor superfamily (TNFRSF) receptor activator of NF-kB (RANK), lymphotoxin β receptor (LtβR), and CD40 in the maturation of mTECs.[1] Still, the molecular determinants that control the function of these key inducers of mTECs remain unknown. Other uncertainties concern the signaling pathways that maintain the multilayered function of TECs in vivo.

The tumor suppressor protein p53 is a recognized regulator of cell-cycle arrest and apoptosis. Yet recent studies have revealed alternative roles for p53 in immunoregulation and autoimmunity.[5] In relation to the thymic epithelium, the observations that the p53 homolog p63 controls the turnover of TEC progenitors[6] imply a possible functional relationship within the p53 family. The analysis of the role of p53 in TEC physiology has been precluded because of its broad expression pattern and the complex phenotype of germline p53-null mice, which ultimately develop thymic lymphomas.[7] Despite such limitations, several studies link p53 to TEC homeostasis. Although germline deletion in wild-type p53-induced phosphatase 1, a p53-target gene, impairs the maturation of mTECs and thymic regeneration,[8] the systemic administration of p53 inhibitors moderately improves

TEC recovery and thymopoiesis following BMT.[9] Because genetically engineered mouse models and pharmacological studies often hide lineage-specific functions of broadly acting genes, the cell-autonomous relevance of p53 in the dynamic differentiation of TECs in vivo remains unexplored. Our findings underscore the requirement for p53 in TECs to support their role in T-cell development and selection.

Methods

All procedures are further detailed in the supplemental Methods section, available on the Blood Web site.

Mice

C57BL/6 $p53^{fl/fl}$, *Foxn1*^{Cre}, and Marilyn-*Rag2*$^{-/-}$ mice[10-12] were housed under specific pathogen-free conditions. Experiments were performed under the European guidelines for animal experimentation.

Flow cytometry

INSTITUTO DE INVESTIGAÇÃO E INOVAÇÃO EM SAÚDE
UNIVERSIDADE DO PORTO

Rua Alfredo Allen, 208
4200-135 Porto
Portugal
+351 220 408 800
info@i3s.up.pt
www.i3s.up.pt

TECs and hematopoietic cells were isolated and stained as described.[12] Cells were analyzed on a fluorescence-activated cell sorter (FACS) Canto II and a LSR Fortessa and sorted on a FACSAria I (BD Biosciences) (purities were >96%). Data were analyzed on FlowJo software.

Histology

Thymic lobes were prepared for immunofluorescence analysis, as described.[12] Paraffin-embedded tissue sections from indicated organs were stained with hematoxylin and eosin (H&E). Analysis was done on a light microscope (Olympus CX31) and IN Cell Analyzer2000 (GE Healthcare). Images were processed using Fiji software.

Gene expression

Messenger RNA (mRNA) isolation and complementary DNA (cDNA) synthesis were done, as described.[12] Real-time polymerase chain reaction (RT-PCR) was performed using TaqMan Universal PCR Master Mix and probes for selected genes.

Fetal thymic organ culture (FTOC)

We established 2-deoxyguanosine (dGuo)-treated FTOC, as described[12] and cultured it in medium alone or with recombinant CD40L (5 μg/mL), agonist antibodies anti-RANK (1 μg/mL) (R&D Systems) or anti-LTβR (10 μg/mL; AC.H6), and Pifithrin-α (50 μg/mL; Sigma-Aldrich).

Luciferase assay

In silico analysis identified putative p53-binding sites in the promoter of *Tnfrsf11a*. p53-Deficient MEFs were transiently cotransfected with a reporter firefly luciferase plasmid containing genomic fragments of *Tnfrsf11a* or *Cdkn1a* promoters along with a p53-expressing vector. Renilla luciferase plasmid was cotransfected as an internal control (Dual-Luciferase Reporter Assay System, Promega).

RNA sequencing

Total RNA library preparation and high-throughput sequencing of sorted cTECs/mTECs samples from p53cKO and control littermates were performed at Gene Core facility (EMBL, Germany). The number of reads per gene was counted using HTSeq-count,[13] and data were analyzed with DESeq2 package.[14] Gene ontology (GO) enrichment analysis was done using a model-based gene set analysis.[15]

Regulatory T-cell suppression assay

Control and p53cKO-derived regulatory T cells were sorted as $CD25^{high}CD4^{+}$ T cells and cocultured with carboxyfluorescein diacetate succinimidyl ester–labeled T cells at various ratios in the presence of anti-CD3 mAb and irradiated splenocytes. The frequency of dividing cells was determined, as described.[16]

Statistical analysis

The 2-tailed Mann-Whitney test was used for statistical differences between groups, and a 2-way analysis of variance was used for multiple comparisons (GraphPad Prism).

INSTITUTO
DE INVESTIGAÇÃO
E INOVAÇÃO
EM SAÚDE
UNIVERSIDADE
DO PORTO

Rua Alfredo Allen, 208
4200-135 Porto
Portugal
+351 220 408 800
info@i3s.up.pt
www.i3s.up.pt

Results

Inactivation of Trp53 in TECs reduces the mTEC compartment

To investigate the function of p53 in the thymic epithelium, we conditionally deleted the p53 gene (*Trp53*) in TECs by crossing mice with loxP-flanked alleles of *Trp53* (*Trp53*$^{fl/fl}$)[10] with mice expressing Cre recombinase under the control of the *Foxn1* promoter (*Foxn1*^{Cre}), which directs the expression of Cre recombinase to virtually all TECs during embryonic and postnatal life.[11] *Foxn1*^{Cre}:*Trp53*$^{fl/fl}$ (p53cKO) mice were born without obvious abnormalities and did not develop spontaneous tumors in the thymus or skin, which also contains Foxn1^{+} keratinocytes.[11] The Cre-mediated deletion of *Trp53*^{fl} allele was detected in TECs but not in thymocytes from p53cKO mice nor in TECs from *Trp53*$^{fl/fl}$ littermate controls (Ctr) (Figure 1A and supplemental Figure 1A-B). Although not statistically different, *Trp53* levels were moderately increased in mTECs in comparison with cTECs from the control thymus (Figure 1B), indicating that p53 is expressed under physiological conditions. The same transcript was nearly absent in cTECs and mTECs from p53cKO mice (Figure 1B) but remained similarly expressed in thymocytes from Ctr and p53cKO mice (supplemental Figure 1C).

We started by comparing the thymic epithelium composition in control and p53cKO mice throughout life. Although with altered proportions in relation to controls, cTEC numbers were normal during fetal, postnatal, and prepuberty periods, becoming moderately diminished in 10-week-old p53cKO mice (Figure 1C-D). In contrast, though seemingly similar to control mice at E16.5, the frequency and numbers of mTECs were continually reduced in mutant mice from the postnatal period onward (Figure 1C-D). Concordantly, the global medullary compartment and the number of UEA^{+}mTECs were reduced in the adult p53cKO thymus, without affecting the compartmentalization into the cortex and medulla (supplemental Figure 1D). We assessed possible Cre-mediated cellular toxicity and found no major changes in thymic and cTEC/mTEC cellularities of *Foxn1*^{Cre}:*Trp53*$^{+/+}$ mice in comparison with *Trp53*$^{+/+}$ mice (supplemental Figure 1E). Age-matched *Trp53*$^{fl/fl}$ littermates were used as controls in subsequent experiments.

The impact of *Trp53* deletion in mTECs led us to examine their differentiation program. First, we subdivided mTECs into CD80^{lo}, which include immature cells and a minor subset of post-Aire terminally differentiated cells in the adult thymus, and mature CD80^{hi}, which contains Aire-expressing cells.[1,17] The development of CD80^{hi} and Aire^{+} mTECs was delayed in the embryonic p53cKO thymus but was normalized to the proportions of the control thymus during prepuberty (Figure 1E). Despite the restoration of complete mTEC differentiation, the number of CD80^{hi} and Aire^{+} mTECs was diminished in p53cKO thymus throughout life, whereas the CD80^{lo} subset became affected only in adult mice(Figure1F). Second, analysis of mTEC turnover revealed an increase in the rate of p53cKO mTECs in active cycling (S/G2/M) (supplemental Figure 1F). Moreover, we monitored the extent of DNA double-strand breaks[18] and apoptosis, and found that the percentages of phosphorylated γ-H2AX and annexin V^{+}, respectively, were slightly increased in p53cKO mTECs, particularly within CD80^{lo} cells (supplemental Figure 1G-H). These findings suggest that increased apoptosis rather than defective proliferation might contribute to the reduced number of mTECs in p53cKO mice. Lastly, analysis of the expression of a panel of TRAs showed that Aire-independent genes were downregulated in p53cKO mTECs, whereas Aire-dependent genes presented a variable pattern in both mTEC subtypes (Figure 1G). Our data suggest that p53 is superfluous for cTEC/mTEC specification but instead controls mTEC homeostasis.

p53 regulates RANK expression in TECs

INSTITUTO DE INVESTIGAÇÃO E INOVAÇÃO EM SAÚDE
UNIVERSIDADE DO PORTO

Rua Alfredo Allen, 208
4200-135 Porto
Portugal
+351 220 408 800
info@i3s.up.pt
www.i3s.up.pt

The similarity between the mTEC-phenotype of p53cKO mice and that of mice with defects in RANK, CD40, and LTβR[19] led us to evaluate whether p53 fine-tunes the expression of these TNFRSF members. Additionally, we analyzed the expression of osteoprotegerin (OPG), a decoy receptor of RANK ligand.[19] Although the levels of *Tnfrsf5* (CD40), *Tnfrsf3* (LTβR), and *Tnfrsf11b* (OPG) were normal, the expression of *Tnfrsf11a* (RANK) was reduced in p53cKO mTECs (Figure 2A). To examine the functional relationship between p53 and RANK, we used well-defined in vitro models of mTEC differentiation, in which E15.5 dGuo-FTOCs were depleted of hematopoietic cells and then stimulated through RANK.[12] Strikingly, the frequency and numbers of mature CD80$^+$ and Aire$^+$ mTECs in RANK-stimulated p53cKO dGuo-FTOCs were reduced in relation to controls (Figure 2B). Contrarily, CD40-mediated mTEC maturation and CD40 expression on p53cKO mTECs were unaffected (supplemental Figure 2A-B). Hence, loss of p53 appeared to specifically dampen in vitro mTEC differentiation induced by RANK. Given that RANK activation induces its own expression,[20] we evaluated whether p53 positively controls this self-amplification loop. Concordantly, RANK-mediated stimulation augmented the expression of *Tnfrsf11a* in TECs from control dGuo-FTOC. Noticeably, this increase was attenuated in TECs from both RANK-activated p53cKO dGuo-FTOC and RANK-activated control dGuo-FTOC cotreated with the p53 inhibitor pifithrin-α (Figure 2C), indicating that p53 controls the expression of *Tnfrsf11a*. In silico analysis identified 6 putative p53 REs[21] within the 4kb region upstream of the transcription start site (TSS) of *Tnfrsf11a* (Figure 2D). We cloned 1kb genomic DNA fragments containing these potential p53 Res (named A-D) into a luciferase reporter plasmid and assessed their p53-mediated transactivation in p53-deficient MEFs, which were cotransfected with a p53-expressing vector. As a positive control, we used a *Cdkn1a* (p21)-derived fragment containing a bona fide p53 RE.[21] Notably, p53 increased luciferase expression driven by *Tnfrsf11a*-derived fragments A, C, and D, but not B (Figure 2D). These results imply that p53 has the potential to control the activity of *Tnfrsf11a* promoter. To study whether p53 was reciprocally induced under mTEC differentiating conditions, we activated control dGuo-FTOCs with RANK, CD40, and LTβR agonists. Contrary to LTβR stimulation, individual RANK- and CD40-engagement induced *Trp53* expression in TECs, an effect that was further augmented by combined activation (Figure 2E). These results indicate that both RANK and CD40 signaling induce p53, which in turn promotes RANK expression and RANK-driven mTEC differentiation.

p53 specifically regulates a broad network of the mTEC transcriptome

Given that p53 governs multiple transcriptional programs in distinct cells,[22-24] we examined its genome-wide influence in TECs. To do so, we performed RNA sequencing (RNA-Seq) analysis and compared the transcriptome of cTECs and mTECs isolated from 2-week-old control and p53cKO mice. We selected this age to permit the maturation of mTEC, the emergence of p53cKO phenotype, and the sufficient abundance of cTEC/mTEC subsets for analysis. The number of genes expressed in the control and p53cKO mTECs was higher than in their cTEC counterparts, resulting in the expected cTEC/mTEC segregation (Figure 3A and supplemental Figure 3A-B). *Trp53* levels were increased in control mTECs and markedly reduced in p53cKO-derived TEC subsets. The expression of cTEC- and mTEC-associated genes separated the 2 lineages independently of their genotype (supplemental Figure 3 C-D), validating the accuracy of sorted samples. Strikingly, though randomly associated within cTEC subsets, the biological replicates of control and p53cKO mTECs defined 2 distinct clusters (Figure 3A). Accordingly, the number of differentially expressed genes between p53cKO and control mTECs was substantially larger than in cTECs (Figure 3B and supplemental Tables 1-2). The identification of 1418 upregulated genes and 1945 downregulated genes in p53cKO mTECs implies that p53 negatively and positively regulates gene expression in mTECs (Figure 3C). Concordant with previous observations, *Tnfrsf11a* expression was reduced in p53cKO mTECs analyzed by RNA-seq and

INSTITUTO
DE INVESTIGAÇÃO
E INOVAÇÃO
EM SAÚDE
UNIVERSIDADE
DO PORTO

Rua Alfredo Allen, 208
4200-135 Porto
Portugal
+351 220 408 800
info@i3s.up.pt
www.i3s.up.pt

quantitative RT-PCR (qRT-PCR) (supplemental Figure 3E). Yet, RANK was not identified among the list of differentially expressed genes most possibly due to the stringent statistical analysis of RNA-Seq, differences in gene normalization, and intrathymic sample variation.

Using a publicly available annotated list of TRA genes,[25] we next cross-examined their representation within differentially expressed genes of p53cKO mTECs. Notably, nearly half of the downregulated genes in p53cKO mTECs comprised purported TRAs, with a similar incidence of Aire-dependent and Aire-independent targets (Figure 3D). The proportion of TRAs within upregulated genes of p53cKO mTECs was lower, including mostly Aire-independent targets (Figure 3D). These data suggest that p53 regulates promiscuous gene expression in mTECs. Additionally, GO enrichment analysis in differentially expressed genes did not reveal any particular term in cTECs but was associated to diverse functional categories in p53cKO mTECs. Specifically, upregulated genes indicated an increase in DNA replication, mitosis, ribosome biogenesis, RNA and protein complex binding, ATPase activity, and constituents of nuclear pore. Conversely, downregulated genes suggested an attenuation in transmembrane transport; actin filament-based process; neuropeptide signaling pathway; carbohydrate and ion binding; and RNAPII transcription factor, enzyme inhibitor, hormone-factor, and growth-factor activity (Figure 3E and supplemental Tables 3-6). Concordant to the mTEC-restricted phenotype of p53cKO mice, these results suggest that p53 controls a multifaceted transcriptional program in mTECs.

Adult p53cKO mice display an impaired regular and regenerative thymopoiesis

We then analyzed how the described changes in TEC microenvironments affected the thymic activity of p53cKO mice. The frequency and abundance of major thymocyte subsets, including early thymic precursors (ETP), double-negative (DN) subsets, and double-positive (DP) and single-positive (SP) CD4 and CD8 cells, were comparable in control and mutant mice during fetal and prepuberty life (Figure 4A-C). Notably, a global deficit in thymopoiesis appeared in 10-week-old p53cKO mice (Figure 4A), without altering the global T-cell differentiation program. Namely, the progression through DN1-DN4 stages and the rate of positive selection, as measured by the frequency of $CD3^{+}CD69^{+}$ thymocytes, were largely similar between the control and p53cKO thymus (Figure4B). However, we found a reduction in the proportion of DN1s and ETPs in the p53cKO thymus (Figure 4B). Correspondingly, the numbers of all major thymic subsets steadily declined in p53cKO mice, this trend being apparent in 6-week-old mice (Figure 4C). These perturbations extended to the peripheral T-cell compartment of adult p53cKO mice, with a reduction in splenic CD4 and CD8 T-cell counts (Figure 4D). The dysfunctional nature of the adult mutant thymus led us to further analyze their regenerative capacity following ionizing radiation. Although numerically different at baseline, mTECs were markedly depleted in both groups 5 days after sublethal total-body irradiation (supplemental Figure 4A). This reduction was attenuated in p53cKO mTECs supplemental Figure 4A), suggesting that ablation of p53 conferred a slight protection to radiation-induced apoptosis. Although the recovery of cTECs was similar in both groups, the restoration of mTEC cellularity, including $CD80^{+}$ and $Aire^{+}$ subsets, was markedly impaired in p53cKO mice (supplemental Figure 4A-C). Additionally, the recovery of thymopoiesis was also significantly compromised in p53cKO mice (Figure 4E), affecting de novo generation of all major thymic subsets (Figure 4F) and the reconstitution of the peripheral T cells (Figure 4G). Our findings indicate that adult p53cKO mice fail to maintain normal and regenerative thymopoiesis.

mTEC-dependent thymopoiesis is compromised in p53cKO mice

INSTITUTO DE INVESTIGAÇÃO E INOVAÇÃO EM SAÚDE
UNIVERSIDADE DO PORTO

Rua Alfredo Allen, 208
4200-135 Porto
Portugal
+351 220 408 800
info@i3s.up.pt
www.i3s.up.pt

As the loss of mTECs preceded the deterioration of thymopoiesis during adulthood, we examined whether the stages of T-cell development that were functionally linked to mTECs[1] were prematurely affected in p53cKO thymus. To survey cortical and medullary clonal deletion, we assessed the frequency of DP and SP4 thymocytes that coexpressed PD-1 and Helios,[26] respectively, and found no major differences between control and p53cKO thymus (Figure 5A). Moreover, we crossed p53cKO mice with Marilyn-Rag2$^{-/-}$ TCR transgenic mice, in which thymocytes express I-A^{b}-restricted HY-specific TCR.[12] Thymocyte development in the p53cKO background reproduced that observed in controls, with a similar number of positively and negatively selected thymocytes in female and male mice, respectively (Figure 5B). In line with the absence of SP4 accumulation at steady state (Figure 4B), these results indicated that negative selection seemed intact in p53cKO mice. Strikingly, analysis of regulatory T-cell differentiation and postselection SP maturation showed a respective decrease in the proportions and numbers of CD25^{+}Foxp3^{+} regulatory T cells and mature CD24^{lo}CD62L^{hi} SP4 thymocytes in mutant thymus (Figure 5 C-D). These findings implicate a requirement for p53 in TECs to maintain continual mTEC-dependent thymopoiesis.

Signs of disturbed peripheral tolerance unfold in p53cKO mice

The alterations in mTECs led us to seek signs of peripheral autoimmune manifestations in mutant mice. We did not detect the presence of autoantibodies against multiple organs (stomach, testis, liver, salivary, and lacrimal glands) in the serum of aged p53cKO mice in comparison with controls (data not shown). Yet larger and more prevalent lymphocytic infiltrations were found in the salivary and lacrimal glands of aged p53cKO mice (Figure 6A-B, supplemental Figure 5A). Despite the reduction in the numbers of thymic regulatory T cells, their frequency in the spleen of adult p53cKO mice was normal (supplemental Figure 5B). However, as total peripheral CD4 T cell counts were reduced (Figure 4D), both conventional and regulatory T cells were diminished in mutant mice (supplemental Figure 5B). Moreover, p53cKO-derived peripheral regulatory T cells suppressed polyclonal T-cell activation in vitro (supplemental Figure 5C), showing a broad intact function and potentially explaining the mild autoimmune manifestations. These findings suggest that the perturbed mTEC niche of p53cKO mice might predispose to defects in tolerance. The development of autoimmunity coupled with defects in mTECs is normally contained in the C56BL/6 background but is potentiated by lymphopenia, as is observed in the case of Aire and XCL1 deficiencies.[27,28] To examine the functional link between scarce mTEC niches and disturbed T-cell tolerance in p53cKO mice, we adoptively transferred thymocytes derived from control and mutant adult thymus into *Rag2*$^{-/-}$ mice and monitored recipient mice for clinical signs of disease. Recipient mice that received p53cKO-derived thymocytes exhibited accelerated weight loss, developed diarrhea and presented lymphocytic infiltration and tissue damage in the colon (Figure 6C). The presence of T cells in the spleen of both groups indicated an effective cell transfer (supplemental Figure 5D). Similar to the analysis at steady state, small lymphocyte infiltrates were also more frequent in the salivary glands of the same group (Figure 6D). Our results indicate that the p53 mutant thymus renders developing T cells more susceptible to failure in establishing peripheral self-tolerance in aged and lymphopenia settings.

Discussion

Our study positions p53 as a prime determinant of mTEC integrity in vivo, mapping a functional link between p53 and RANK in mTECs. This was manifested by a reduced RANK-driven mTEC induction in the p53cKO thymus in vitro, an observation that curiously mirrored the delayed appearance of embryonicp53cKO mature mTECs in vivo. We found that mTECs express higher

INSTITUTO
DE INVESTIGAÇÃO
E INOVAÇÃO
EM SAÚDE
UNIVERSIDADE
DO PORTO

Rua Alfredo Allen, 208
4200-135 Porto
Portugal
+351 220 408 800
info@i3s.up.pt
www.i3s.up.pt

levels of p53 than do cTECs and that p53 was reciprocally induced following RANK and CD40 stimulation. These results are consistent with previous studies coupling p53 induction to the NFkB pathway,[29] which is in turn engaged by mTEC-inducing TNFRSF signaling.[19] Yet the reduction in mTECs of p53cKO mice was not as severe as that reported in RANK-deficient mice.[19] The differentiation of mTECs depends on the coordinated action of RANK, CD40, and LTβR signaling.[1] It is conceivable that compensatory signals via CD40 and LTβR contribute to the mTEC maturation program of p53cKO mice. Hence, p53 seems to fine-tune, rather than determine, RANK signaling in mTECs, cooperating in a functional feed-forward loop to sustain the medullary epithelial compartment.

Our results suggest that p53 functions as a molecular hub in mTECs, regulating a wide transcriptional program that extends beyond balancing RANK expression. Typically, p53 is maintained at low levels under steady-state conditions, being activated in response to various stress signals.[21] Nonetheless, p53 also has basal transcriptional functions in unstressed cells.[23] Apart from RANK and CD40, it is possible that additional extrinsic and intrinsic cues generated within the thymus trigger a p53-driven response in mTECs. Although the mechanisms that induce p53 in mTECs remain elusive, our observations argue that its activity is not dormant. Genome-wide chromatin-binding approaches revealed extensive and distinct cell-specific p53-driven transcription programs,[22-24] indicating that p53-mediated gene expression is context dependent. We found that p53 controls a broad set of genes linked to core processes in mTEC biology, which are not related to other well-known mechanisms controlling mTEC maintenance. The increased apoptosis susceptibility of p53-deficient mTECs might be a corollary of these broad alterations, possibly explaining the reduced mTEC compartment of p53cKO mice. Yet the presumed asynchrony of apoptosis at a population level and the rapid clearance of dying cells may confound measurements of cell death in vivo. Moreover, it remains to be determined whether differentially expressed genes are directly regulated by p53 or indirectly influenced through the perturbation of downstream genes of the p53-induced pathway. Further studies should elucidate the individual contribution of these gene products or processes to the maintenance of mTEC homeostasis and their homo and heterotypic cellular interactions within the thymus. It is also important to consider that the hyperactive transcriptional state of mTECs might facilitate the accessibility of p53 to its target genes. The large prevalence of TRAs among the differentially expressed genes of p53cKO mTECs suggests that p53 influences promiscuous gene expression. Still, the expression of Aire[25] and Fezf[24] was normal in p53cKO mTECs. Because mTECs express clusters of TRAs at a single-cell level,[3,30] the reduction in TRAs might alternatively reflect an underrepresentation of certain mTEC subsets in mutant thymus.

The disruption in the mTEC niche appeared to spread to the cTEC compartment in the adult p53cKO mice, evolving to a global failure in regular and regenerative thymopoiesis. The deficit in thymic activity extended to a decrease in splenic T cells, reinforcing the notion that peripheral T-cell homeostasis in mice also depends on regular thymic output.[31] Thus, the sustainability of the mTEC niche seems to be a deterministic factor in regulating thymic function. How the changes in mTECs are reflected in the cortex is intriguing. The phenotype and transcriptional profile of cTECs, as well as the early T-cell development and positive selection, were apparently normal in p53cKO mice. Yet we cannot formally exclude that p53 directly regulates cTEC homeostasis later in life. Alternatively, changes in mTECs might perturb the corticomedullary junction and cortex, thereby limiting the number of BM-derived thymic progenitors and the magnitude of premedullary stages of T-cell differentiation. Accordingly, the numbers of ETPs, DN, and DP thymocytes were diminished in aged p53cKO mice, providing a possible explanation for thymic hypoplasia. These findings could implicate the existence of a complex functional and structural interplay between TEC and nonepithelial cell subsets (eg, endothelia and mesenchyme) in balancing thymopoiesis.

INSTITUTO
DE INVESTIGAÇÃO
E INOVAÇÃO
EM SAÚDE
UNIVERSIDADE
DO PORTO

Rua Alfredo Allen, 208
4200-135 Porto
Portugal
+351 220 408 800
info@i3s.up.pt
www.i3s.up.pt

The contracted mTEC compartment of p53cKO mice was physiologically linked to abnormalities in mTEC-dependent regulatory T-cell differentiation and SP maturation, providing a possible molecular explanation for the signs of deregulated immunological tolerance in mutant mice. Albeit negative selection seemed normal at a polyclonal level, we cannot exclude the possibility that rare autoreactive thymocytes escape from the p53cKO thymus. In line with previous studies,[32] we reason that the underrepresentation of regulatory T cells and mature SP4 represents the footprint of a decrease in the availability of mTEC niches. Concordantly, mild signs of autoimmune manifestations unfolded in aged p53cKO mice and in immunodeficient mice receiving p53cKO-derived thymocytes. Although we did not provide a direct link between the disturbed tolerance and the deficiency in regulatory T- cell numbers or their specificities and the specificities of conventional T cells, our findings suggest that the insufficient mTEC niche of p53cKO mice predisposes to defects in immune tolerance under lymphopenia. Also, the signs of abnormal immunological tolerance in p53cKO mice were weaker in comparison with other mTEC-deficient conditions.[19] We reason that the remaining mTEC niche of mutant thymus, together with the genetic background and extrathymic compensatory mechanisms, allows the establishment of peripheral tolerance during the first weeks of age, a period that is sufficient to prevent the development of autoimmunity.[33] Future studies should identify the distinct contribution of altered thymic and peripheral T-cell subsets to the disturbed tolerance induction of mutant mice.

Beyond positioning p53 as a novel guardian of thymus function, our findings are also of clinical relevance and reinforce the notion of a modulatory role for p53 in immune homeostasis and autoimmunity.[5] Moreover, the use of p53 inhibitors, such as Pifithrin-β, has been approved in clinical trials to attenuate the side effects of chemotherapy.[9] Given the described adverse impact of disrupting p53 in TECs and in T cells,5 the therapeutic use of p53 inhibitors must be implemented with care to safeguard the balance between immune reconstitution and tolerance induction.

Acknowledgments

The authors thank Thomas Boehm (Max Planck Institute of Immunology and Epigenetics) for Foxn1-Cre mice; Rui Appelberg (I3S) and Nuno Rodrigues dos Santos (I3S) for critical reading of the manuscript; Matthias Futschik and José Pedro Pinto (University of Algarve) for critical discussions; and Sofia Lamas, Rui Fernandes, Catarina Leitão, and the caretakers from the animal facility for technical assistance.

This study was supported by the European Research Council (ERC) under the European Union's Horizon 2020 research and innovation program (grant agreement No 637843-TEC_Pro) starting grant attributed to N.L.A., by FEDER (Fundo Europeu de Desenvolvimento Regional) funds through the Operational Competitiveness Programme–COMPETE, and by National Funds through Fundação para a Ciência e a Tecnologia (FCT) under the project FCOMP-01-0124-FEDER-021075 (PTDC/SAU-IMU/117057/2010), by NORTE-01-0145-FEDER-000012–Structured program on bioengineered therapies for infectious diseases and tissue regeneration, supported by Norte Portugal Regional Operational Programme (NORTE 2020), under the PORTUGAL 2020 Partnership Agreement, through the European Regional Development Fund (FEDER); by FEDER funds through the COMPETE 2020–Operational Programme for Competitiveness and Internationalisation (POCI), Portugal 2020, and by Portuguese funds through FCT/Ministério da Ciência, Tecnologia e Inovação in the framework of the project Institute for Research and Innovation in Health Sciences (POCI-01-0145-FEDER-007274). The Investigator Program and doctoral and postdoctoral fellowships from FCT support N.L.A., P.M.R., A.R.R., I.P.-C., and C.M.

INSTITUTO
DE INVESTIGAÇÃO
E INOVAÇÃO
EM SAÚDE
UNIVERSIDADE
DO PORTO

Rua Alfredo Allen, 208
4200-135 Porto
Portugal
+351 220 408 800
info@i3s.up.pt
www.i3s.up.pt

Authorship

Contribution: N.L.A. conceived and performed the experiments, wrote the manuscript, and secured funding; P.M.R. conceived and performed the experiments and wrote the manuscript; A.R.R., C.P., L.A., J.J.M.L., V.B., I.P.-C., H.X.-F., and C.M. performed the experiments; and A.M. provided expertise and feedback.

Conflict-of-interest disclosure: The authors declare no competing financial interests.

ORCID profiles: N.L.A., 0000-0002-1567-8389.

References

1. Anderson G, Takahama Y. Thymic epithelial cells: working class heroes for T cell development and repertoire selection. Trends Immunol. 2012;33(6): 256-263.

2. Kyewski B, Klein L. A central role for central tolerance. Annu Rev Immunol. 2006;24:571-606.

3. Meredith M, Zemmour D, Mathis D, Benoist C. Aire controls gene expression in the thymic epithelium with ordered stochasticity. Nat Immunol. 2015;16(9):942-949.

4. Takaba H, Morishita Y, Tomofuji Y, et al. Fezf2 orchestrates a thymic program of self-antigen expression for immune tolerance. Cell. 2015; 163(4):975-987.

5. Munoz-Fontela C, Mandinova A, Aaronson SA, Lee SW. Emerging roles of p53 and other tumour-suppressor genes in immune regulation. Nat Rev Immunol. 2016;16(12):741-750.

6. Senoo M, Pinto F, Crum CP, McKeon F. p63 is essential for the proliferative potential of stem cells in stratified epithelia. Cell. 2007;129(3): 523-536.

7. Murray-Zmijewski F, Slee EA, Lu X. A complex barcode underlies the heterogeneous response of p53 to stress. Nat Rev Mol Cell Biol. 2008;9(9): 702-712.

8. Sun L, Li H, Luo H, et al. Phosphatase Wip1 is essential for the maturation and homeostasis of medullary thymic epithelial cells in mice. J Immunol. 2013;191(6):3210-3220.

9. Kelly RM, Goren EM, Taylor PA, et al. Short-term inhibition of p53 combined with keratinocyte growth factor improves thymic epithelial cell recovery and enhances T-cell reconstitution after murine bone marrow transplantation. Blood. 2010; 115(5):1088-1097.

10. Marino S, Vooijs M, van Der Gulden H, Jonkers J, Berns A. Induction of medulloblastomas in p53-null mutant mice by somatic inactivation of Rb in the external granular layer cells of the cerebellum. Genes Dev. 2000;14(8):994-1004.

11. Soza-Ried C, Bleul CC, Schorpp M, Boehm T. Maintenance of thymic epithelial phenotype requires extrinsic signals in mouse and zebrafish. J Immunol. 2008;181(8):5272-5277.

12. Ribeiro AR, Rodrigues PM, Meireles C, Di Santo JP, Alves NL. Thymocyte selection regulates the homeostasis of IL-7-expressing thymic cortical epithelial cells in vivo. J Immunol. 2013;191(3): 1200-1209.

13. Anders S, Pyl PT, Huber W. HTSeq—a Python framework to work with high-throughput sequencing data. Bioinformatics. 2015;31(2): 166-169.

14. Love MI, Huber W, Anders S. Moderated estimation of fold change and dispersion for RNA-seq data with DESeq2. Genome Biol. 2014; 15(12):550.

15. Bauer S, Gagneur J, Robinson PN. Going Bayesian: model-based gene set analysis of genome-scale data. Nucleic Acids Res. 2010;38(11):3523-3532.

16. Alves NL, Hooibrink B, Arosa FA, van Lier RA. IL-15 induces antigen-independent expansion and differentiation of human naive CD81 T cells in vitro. Blood. 2003;102(7):2541-2546.

17. Gray DH, Seach N, Ueno T, et al. Developmental kinetics, turnover, and stimulatory capacity of thymic epithelial cells. Blood. 2006;108(12):3777-3785.

18. Abramson J, Giraud M, Benoist C, Mathis D. Aire's partners in the molecular control of immunological tolerance. Cell. 2010;140(1): 123-135.

19. Irla M, Hollander G, Reith W. Control of central self-tolerance induction by autoreactive CD4+ thymocytes. Trends Immunol. 2010;31(2):71-79.

20. Mouri Y, Yano M, Shinzawa M, et al. Lymphotoxin signal promotes thymic organogenesis by eliciting RANK expression in the embryonic thymic stroma. J Immunol. 2011;186(9):5047-5057.

21. Vousden KH, Prives C. Blinded by the light: the growing complexity of p53. Cell. 2009;137(3): 413-431.

22. Li M, He Y, Dubois W, Wu X, Shi J, Huang J. Distinct regulatory mechanisms and functions for p53-activated and p53-repressed DNA damage response genes in embryonic stem cells. Mol Cell. 2012;46(1):30-42.

23. Kenzelmann Broz D, Spano Mello S, Bieging KT, et al. Global genomic profiling reveals an extensive p53-regulated autophagy program contributing to key p53 responses. Genes Dev. 2013;27(9):1016-1031.

24. Liu Y, Elf SE, Miyata Y, et al. p53 regulates hematopoietic stem cell quiescence. Cell Stem Cell. 2009;4(1):37-48.

25. Sansom SN, Shikama-Dorn N, Zhanybekova S, et al. Population and single-cell genomics reveal the Aire dependency, relief from Polycomb silencing, and distribution of self-antigen expression in thymic epithelia. Genome Res. 2014;24(12):1918-1931.

26. Daley SR, Hu DY, Goodnow CC. Helios marks strongly autoreactive CD41 T cells in two major waves of thymic deletion distinguished by induction of PD-1 or NF-kB. J Exp Med. 2013; 210(2):269-285.

27. Anderson MS, Venanzi ES, Klein L, et al. Projection of an immunological self shadow within the thymus by the Aire protein. Science. 2002; 298(5597):1395-1401.

28. Lei Y, Ripen AM, Ishimaru N, et al. Aire-dependent production of XCL1 mediates medullary accumulation of thymic dendritic cells and contributes to regulatory T cell development. J Exp Med. 2011;208(2):383-394.

29. Perkins ND. Integrating cell-signalling pathways with NF-kappaB and IKK function. Nat Rev Mol Cell Biol. 2007;8(1):49-62.

30. Brennecke P, Reyes A, Pinto S, et al. Single-cell transcriptome analysis reveals coordinated ectopic gene-expression patterns in medullary thymic epithelial cells. Nat Immunol. 2015;16(9): 933-941.

31. Almeida AR, Borghans JA, Freitas AA. T cell homeostasis: thymus regeneration and peripheral T cell restoration in mice with a reduced fraction of competent precursors. J Exp Med. 2001; 194(5):591-599.

32. Cowan JE, Parnell SM, Nakamura K, et al. The thymic medulla is required for Foxp31 regulatory but not conventional CD41 thymocyte development. J Exp Med. 2013;210(4):675-681.

33. Guerau-de-Arellano M, Martinic M, Benoist C, Mathis D. Neonatal tolerance revisited: a perinatal window for Aire control of autoimmunity. J Exp Med. 2009;206(6):1245-1252.

INSTITUTO
DE INVESTIGAÇÃO
E INOVAÇÃO
EM SAÚDE
UNIVERSIDADE
DO PORTO

Rua Alfredo Allen, 208
4200-135 Porto
Portugal
+351 220 408 800
info@i3s.up.pt
www.i3s.up.pt

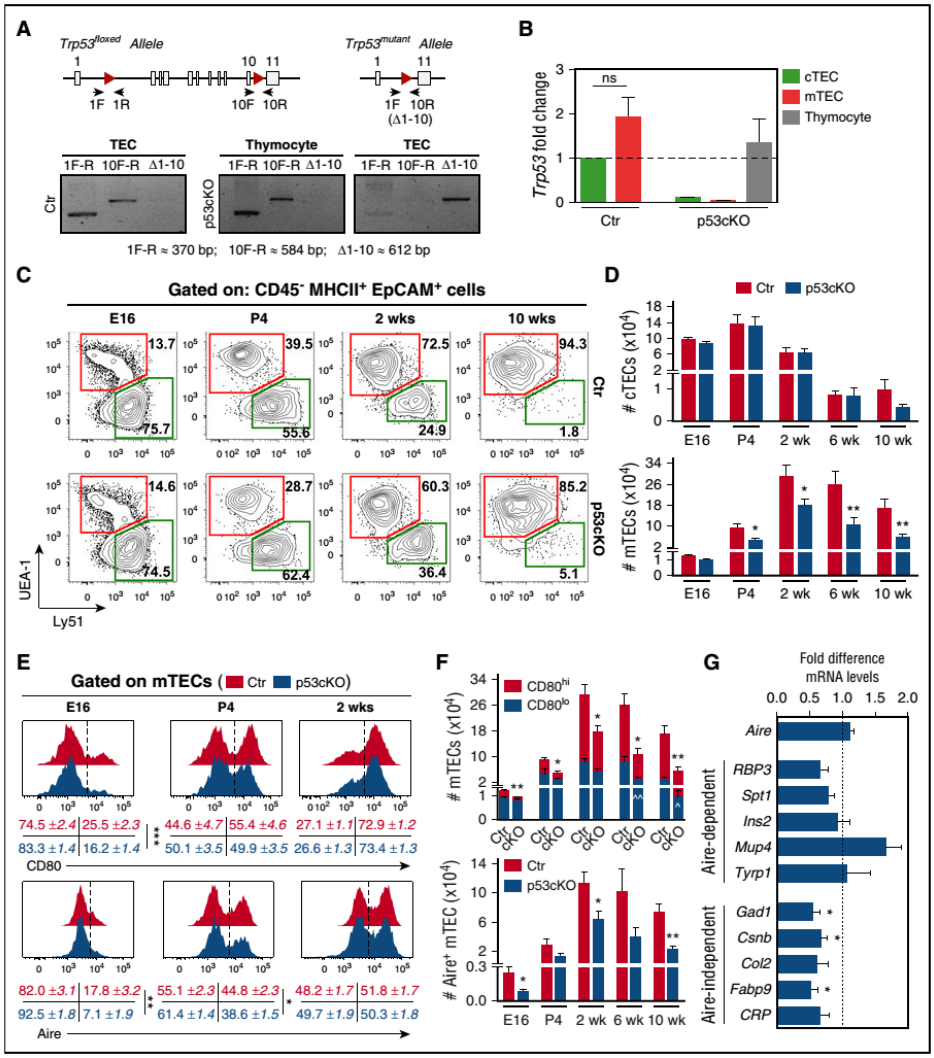

Figure 1. Ablation of *Trp53* in TECs diminishes the size of the mTEC niche. (A) Diagram of the genomic floxed and targeted *Trp53* alleles (top). *LoxP* sequences flank exons 2 through 10 (arrowheads). Examination of Foxn1:Cre-driven deletion of *Trp53* floxed allele by genomic PCR analysis (bottom) in FACS-sorted TECs (CD45$^-$EpCAM$^+$ MHCII$^+$) from Ctr mice and thymocytes (CD45$^+$) and TECs from p53cKO mice at 2 weeks of age, using the depicted primers (1F, 1R, 10F, and 10R). (B) qRT-PCR analysis of *Trp53* expression in FACS-sorted cTECs (UEA$^-$Ly51$^+$), mTECs (UEA$^+$Ly51$^-$), and thymocytes from 2-week-old Ctr and p53cKO mice. Products were detected by amplification of cDNA sequence-spanning exons 5 and 6. Values were normalized to *18s* ribosomal RNA. Values from Ctr cTECs were set as 1, and the fold change in *Trp53* was calculated in relation to the other subsets (mean ± standard error of the mean [SEM], representative of 4 independent experiments). (C-D) The composition of TECs was analyzed at the indicated time points. Flow cytometry analysis of cTECs and mTECs. Dot plots show representative Ly51/UEA staining in TECs (C). Average cellularity of cTECs (top) and mTECs (bottom) (D). Graphs represent data from 2 to 4 independent experiments per time point (n = 5 to 17 per group). (E) Expression of CD80 and Aire in mTECs of Ctr and p53cKO mice at the indicated time points. Numbers represent the average percentages (±SEM) of the gated mTEC subsets. (F) Average cellularity of the mTEC subsets depicted in panel E. Carats and asterisks (^ and *) compare immature and mature mTECs, respectively. The results in panels E and F are shown as mean ± SEM of 5 to 17 mice per group from 3 to 4 independent experiments. (G) Expression of Aire-dependent and Aire-independent TRAs measured by qRT-PCR in FACSsorted mTECs from 2-week-old Ctr and p53cKO mice. Values were normalized to *18s* ribosomal RNA, and those in Ctr mTECs were set as 1. Graphs represent data from 3 independent experiments (mean ± SEM). ns, not significant; wk, week. */^P < .05; **/^^P < .01; ***P < .001.

INSTITUTO DE INVESTIGAÇÃO E INOVAÇÃO EM SAÚDE
UNIVERSIDADE DO PORTO

Rua Alfredo Allen, 208
4200-135 Porto
Portugal
+351 220 408 800
info@i3s.up.pt
www.i3s.up.pt

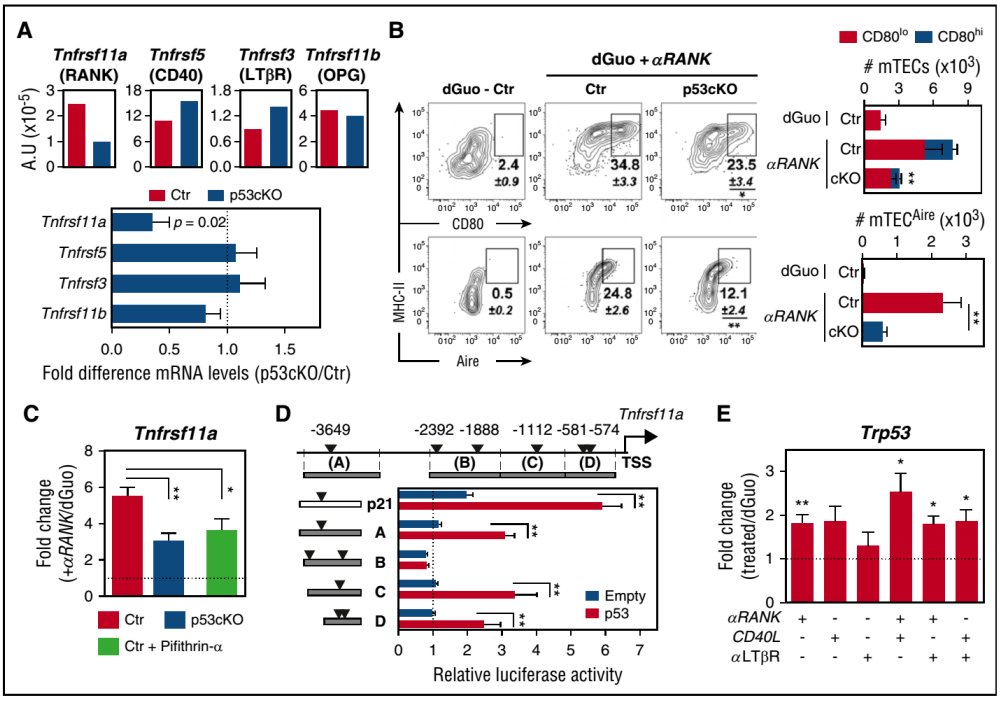

Figure 2. Ablation of *Trp53* in TECs limits the expression and responsiveness of RANK. (A) The expression of *Tnfrsf11a*, *Tnfrsf5*, *Tnfrsf3*, and *Tnfrsf11b* was assessed by qRT-PCR in FACS-sorted mTECs (UEA$^+$Ly51$^-$) from 2-week-old Ctr and p53cKO mice. Values were normalized to *18s* ribosomal RNA. Graphs represent data from 4 independent experiments (top). Fold difference in the relative mRNA levels between Ctr (dashed line) and p53cKO mTECs (bottom). (B) E15.5 dGuo-treated FTOCs from Ctr and p53cKO mice were cultured for 4 days with anti-RANK (αRANK). Expression of CD80 and Aire was analyzed in mTECs (UEA$^+$Ly51$^-$) by flow cytometry. Numbers indicate the mean percentage of gated cells. Graphs show the cellularity of mTEC subsets per thymic lobe. Number of asterisks compare mature mTECs from Ctr with p53cKO mice (top). Results are presented as mean ± SEM of 10 to 12 thymic lobes per group from 5 independent experiments. (C) The expression of *Tnfrsf11a* was analyzed by qRT-PCR in FACS-sorted TECs from Ctr and p53cKO E15.5 dGuo-treated FTOC stimulated over 24 hours with αRANK or αRANK plus Pifithrin-α. Values were normalized as in panel A, and those in TECs from nonstimulated dGuo-treated FTOC were set to 1. Graphs represent data from 3 to 6 independent experiments (mean ± SEM). (D) The region upstream of the *Tnfrsf11a* (RANK) TSS contains putative p53 response elements (REs) (triangles), identified on the basis of the p53 RE matrix logo (RRRC-A/T-A/T-GYYY motifs, in which R is a purine and Y is a pyrimidine) (MatInspector, rVista, or both, software tolls). DNA fragments (A-D) from the *Tnfrsf11a* (RANK) and *Cdkn1a* (p21) loci were cloned into the pGL3-Promoter reporter plasmid. p53 KO MEFs were transiently transfected with the indicated luciferase plasmids along with a p53 overexpressing construct (p53) or an empty construct (Empty). Luciferase reporter activity was normalized to the relative pGL3-promoter signal. Represented is the average of 3 independent experiments (±SEM). (E) The expression of *Trp53* was analyzed by qRT-PCR in FACS-sorted TECs from Ctr and p53cKO E15.5 dGuo-treated FTOC stimulated over 24 hours with anti-RANK, recombinant CD40L, and anti-LTβR at different combinations. Values were normalized as in panel A, and those in TECs from nonstimulated dGuo-treated FTOC were set to 1. Data are representative of 4 independent experiments (mean ± SEM). A.U., arbitrary units; MHC, major histocompatibility complex. *P < .05; **P < .01.

INSTITUTO DE INVESTIGAÇÃO E INOVAÇÃO EM SAÚDE
UNIVERSIDADE DO PORTO

Rua Alfredo Allen, 208
4200-135 Porto
Portugal
+351 220 408 800
info@i3s.up.pt
www.i3s.up.pt

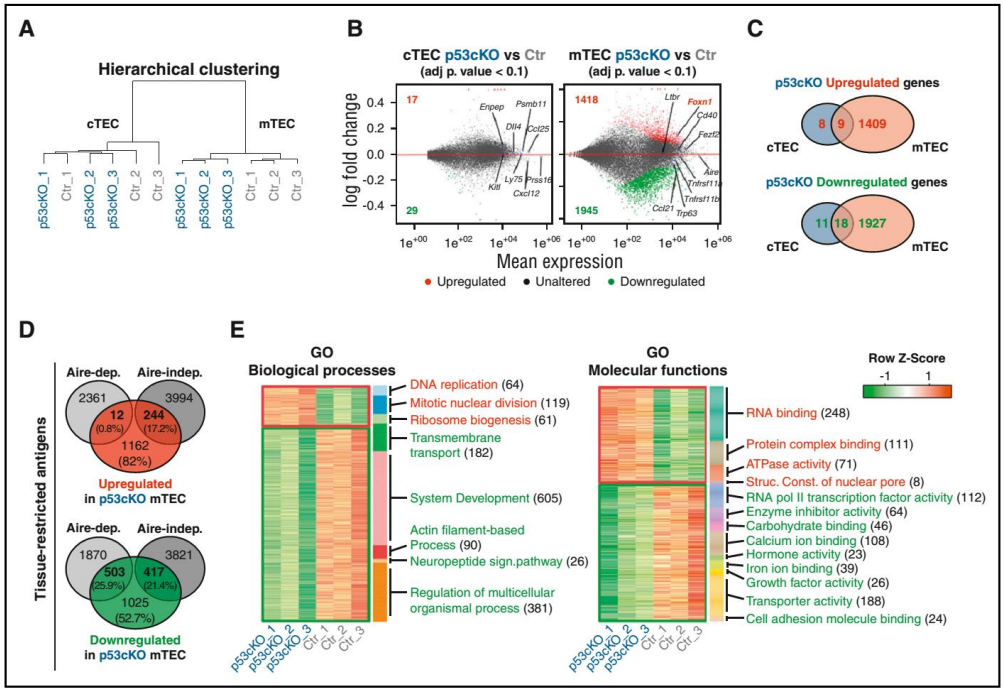

Figure 3. Impact of p53 in the transcriptome of cTECs and mTECs. RNA-Seq analysis of FACS-sorted cTECs and mTECs purified from 2-week-old Ctr and p53cKO mice, including 3 biological replicates per subset. (A) Hierarchical clustering of all samples by gene expression correlation distance for the top 1000 most diverse genes. (B) Comparison of the transcriptome of cTECs from p53cKO versus Ctr mice (left) and mTECs from p53cKO versus Ctr mice (right). Minus-average plots showed the log2-fold change (y-axis) versus the mean expression (x-axis) of total genes obtained by comparison. Genes with a log2-fold change that present an adjusted *P* value that is <0.1 were called differentially expressed (DE). Upregulated and downregulated DE genes in p53cKO samples are highlighted in red and green, respectively, together with their numbers. Unaltered genes are depicted in gray. (C) Venn diagrams represent the number of upregulated (top) or downregulated (bottom) DE genes in cTECs (blue) and mTECs (salmon) of p53cKO versus Ctr mice. (D) Venn diagrams show the number and proportion of upregulated (red) and downregulated (green) genes of p53cKO mTECs within Aire-dependent or Aire-independent TRA genes, as defined by Sansom et al.[25] (E) Heat map of enriched biological processes (left) and molecular functions (right) in upregulated (red) or downregulated (green) DE genes of p53cKO mTECs. Represented are activated (red) or inhibited (green) categories with a marginal posterior probability estimate that is >0.65. In parentheses are indicated the number of DE genes per GO category. Adj p, adjusted *P*; Aire-dep, Aire-dependent; Aire-indep, Aire-independent; ATP, adenosine triphosphate; Struc. Const., structural constituent.

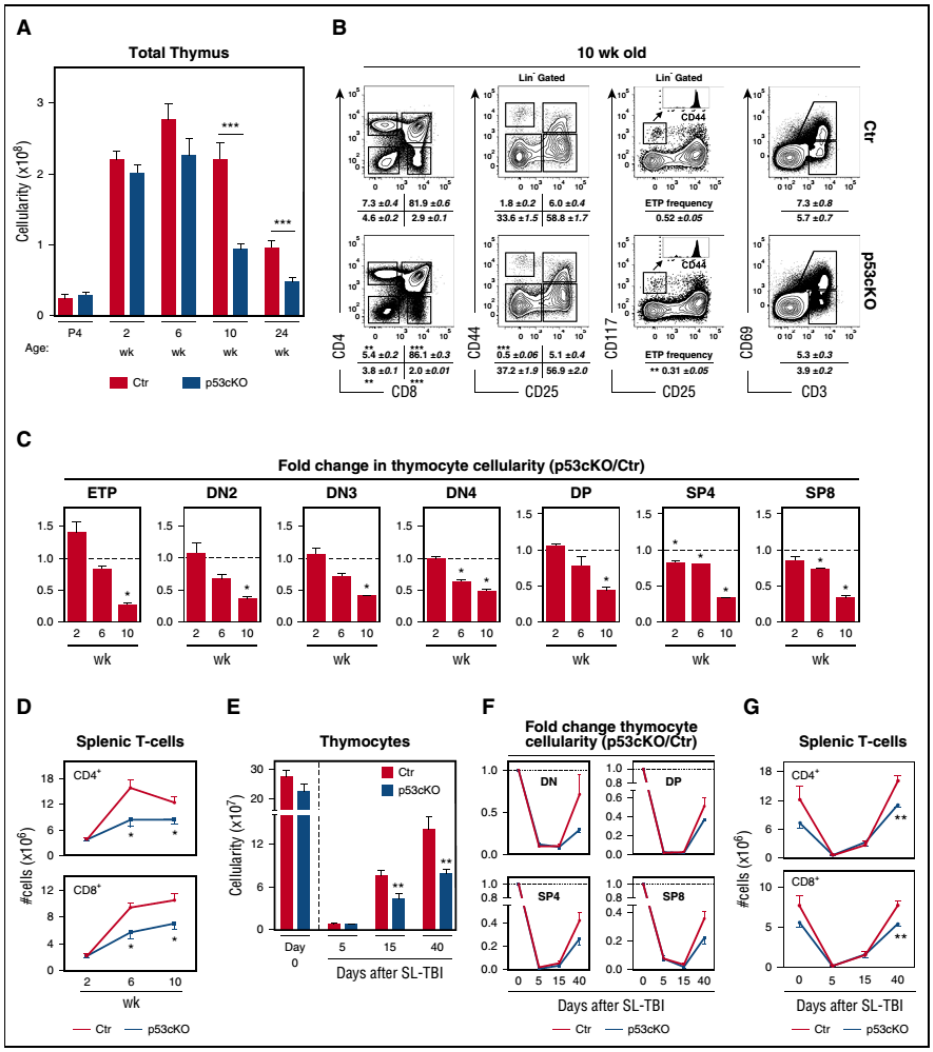

Figure 4. Altered thymopoiesis in p53cKO mice. (A) Thymic cellularity of Ctr and p53cKO mice at various ages. (B) Flow cytometry analysis of T-cell development in 10-week-old Ctr and p53cKO thymus: CD4/CD8 expression on total thymocytes (left); CD44/CD25 expression on DN thymocytes (gated on Lin⁻ cells) (middle left); CD177/CD25 expression on DN thymocytes (gated on Lin⁻ cells) (middle right). ETPs are defined as Lin⁻ CD177⁺CD44⁺CD25⁻; CD69/CD3 expression on total thymocytes (right). Numbers indicate the frequencies of the different subsets (mean ± SEM). (C) Fold change in the number of the indicated thymocyte subsets. For each time point, the values of Ctr mice were set as 1 (dashed line) and compared in relation to p53cKO mice. Graphs represent data from 2 to 3 experiments per time point (n = 6 to 8 mice per group; mean ± SEM). (D) Absolute number of splenic CD4⁺ and CD8⁺ T cells in Ctr and p53cKO mice at different time points. (E) Thymocyte cellularity of sublethally irradiated 6-week-old Ctr and p53cKO mice at the indicated time points posttreatment. (F) Fold change in the cellularity of the thymocyte subsets following sublethal total-body irradiation (SL-TBI). For each time point, the values of nonirradiated Ctr or p53cKO mice were set as 1 (dotted line) and to the ones obtained for SL-TBI Ctr and p53cKO thymus, respectively, at each time point. (G) Numbers of splenic CD4⁺ and CD8⁺ T cells in Ctr and p53cKO mice after SL-TBI. SL-TBI, sublethal total-body irradiation. *P < .05; **P < .01; ***P < .001.

INSTITUTO
DE INVESTIGAÇÃO
E INOVAÇÃO
EM SAÚDE
UNIVERSIDADE
DO PORTO

Rua Alfredo Allen, 208
4200-135 Porto
Portugal
+351 220 408 800
info@i3s.up.pt
www.i3s.up.pt

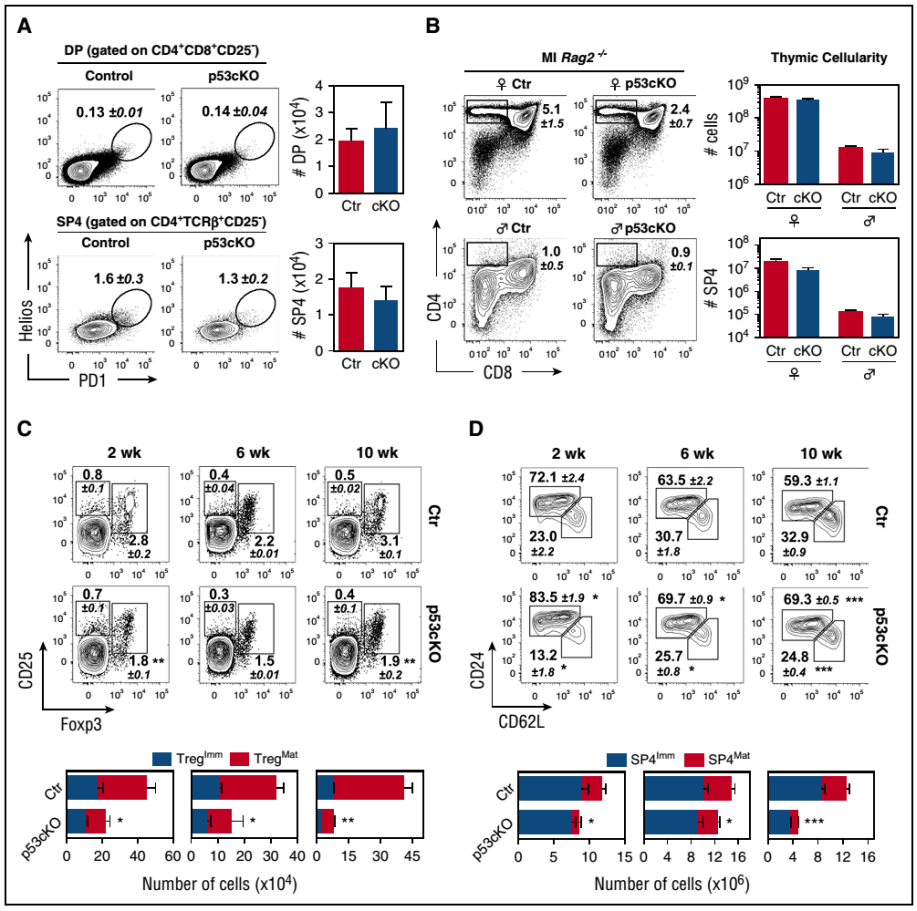

Figure 5. Loss of p53 in TECs reduces specific mTEC-mediated functions. (A) DP (TCRβ⁺CD4⁺CD8⁺CD25⁻) and SP4 (TCR β⁺CD4⁺CD8⁻CD25⁻) thymocytes isolated from 8-week-old Control (Ctr) and p53cKO mice were analyzed for the expression of Helios and PD1. Numbers indicate the mean percentage of gated cells. Graphs show the total number of Helios⁺PD1⁺ thymocytes within the DP and SP4 stage and represent data from 2 independent experiments (n = 4 to 5 mice per group; mean ± SEM). (B) Flow cytometry analysis of thymic selection in 8-week-old female and male Ctr and p53cKO Marilyn-*Rag2*$^{-/-}$ thymus. Numbers indicate the frequencies of SP4 thymocytes (mean ± SEM). Thymic cellularity (top) and the number of SP4 thymocytes (bottom) are depicted on the graphs. Data represent the average of 3 independent experiments (n = 5 to 6 mice per group; mean ± SEM). (C-D) SP4 thymocytes (CD8⁺CD4⁺TCRβ⁺) were analyzed for the expression of CD25 and Foxp3 (C) and CD24 and CD62L (D) at the indicated time points. Numbers indicate the average percentage of gated cells (±SEM). Graphs represent the number of immature (CD25⁺Foxp3⁻) and mature (CD25⁺Foxp3⁺) regulatory T cells (Tregs) (left) (C); the number of immature (CD24^{hi}CD62L^{low}) and mature (CD24^{low}CD62L^{hi}) SP4 thymocytes (right) (D). The asterisk compares mature Treg and mature SP4 cells between Ctr and p53cKO mice. In panels C-D, graphs represent data from 3 independent experiments (n = 4 to 13 mice per group). Results are presented as mean ± SEM. Ml, Marilyn-*Rag2*$^{-/-}$ thymus. ♀, female; ♂, male; *P < .05; **P < .01; ***P < .001.

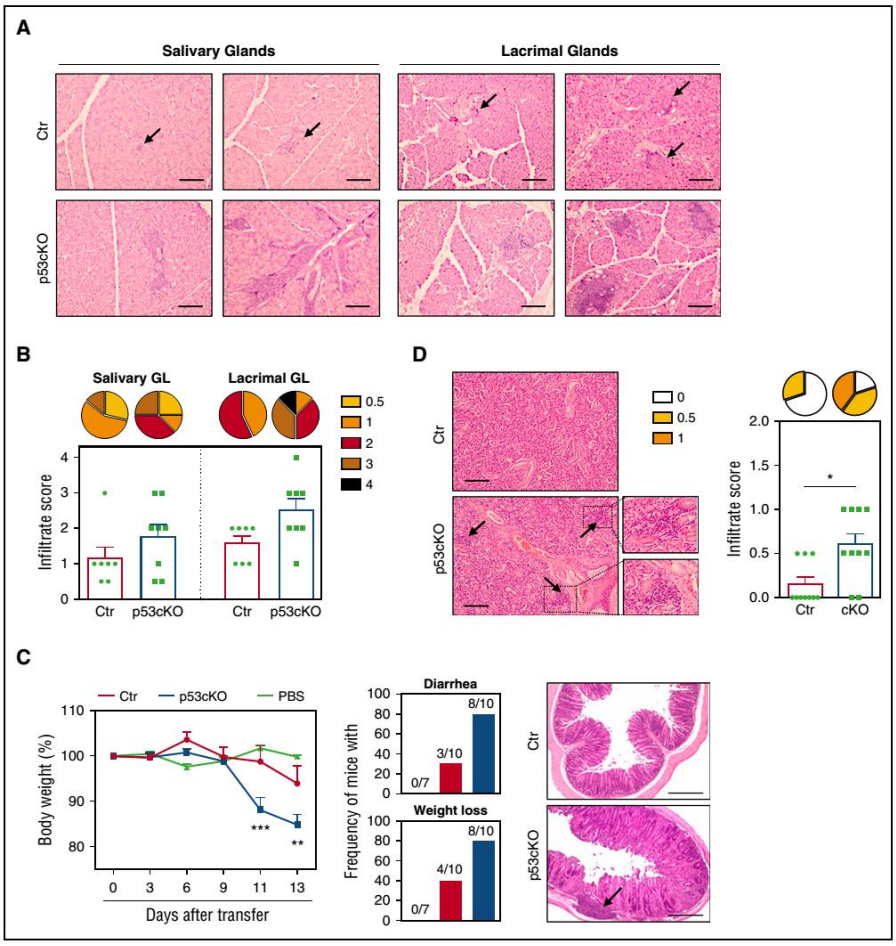

Figure 6. TEC-specific deletion of p53 affects the establishment of peripheral T-cell tolerance. (A) Representative analysis (H&E staining) of the salivary and lacrimal glands obtained from 6- to 7-month-old Ctr and p53cKO mice. (B) Histological scores of inflammatory infiltrates. Pie graphs show the frequency of inflammatory lesions according to their severity. (C) Thymocytes from 10-week-old Ctr (red line) and p53cKO (blue line) mice were intravenously transferred into *Rag2*$^{-/-}$ mice. As a control, *Rag2*$^{-/-}$ mice were treated with phosphate-buffered saline (green line). Change in the body weight of *Rag2*$^{-/-}$ recipients after thymocyte transfer (left). Incidence of diarrhea and weight loss, with the indicated number of recipient mice that develop symptoms (middle). Images show the histological analysis (H&E staining) of the colon of the *Rag2*$^{-/-}$ recipients 14 days after transfer (right). (D) Histological analysis and inflammatory score of the salivary glands. Pie graphs represent the frequency of inflammatory lesions according to their severity. Arrows in panels A, C, and D outline lymphocytic infiltrates. Results are presented as mean ± SEM. Scale bars, 100 μm. PBS, phosphate-buffered saline. *P < .05; **P < .01; ***P < .001.